PNAS
www.pnas.org

Supplementary Information for

NURR1 activation in skeletal muscle controls systemic energy homeostasis and mimics exercise

Leonela Amoasii, Efrain Sanchez-Ortiz, Teppei Fujikawa, Joel K. Elmquist, Rhonda Bassel-Duby and Eric N. Olson

Corresponding author: Eric N. Olson, Ph.D.
E-mail: Eric.Olson@utsouthwestern.edu

This PDF file includes:

Figs. S1 to S7
Table S1

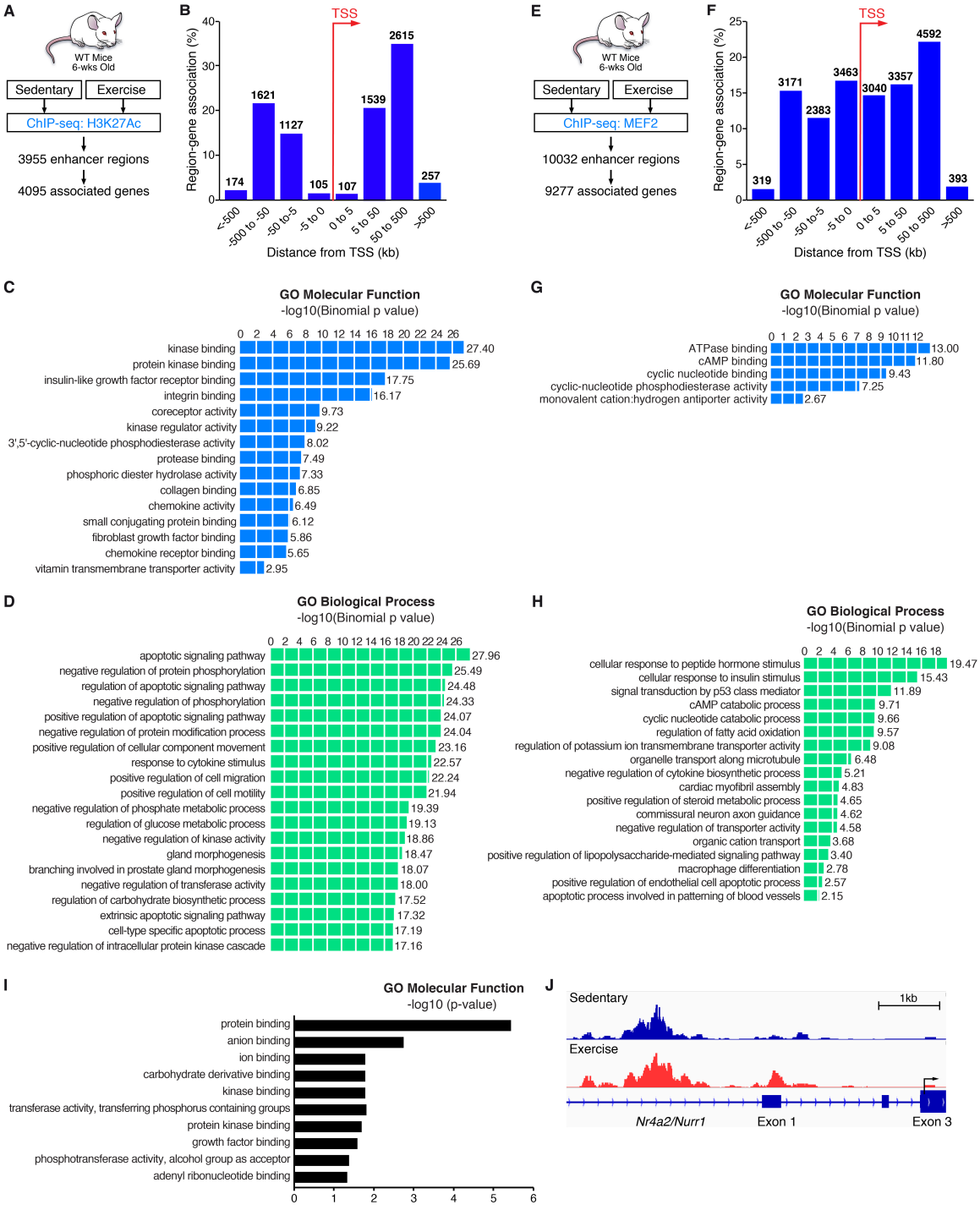
A
WT Mice
6-wks Old
Sedentary
Exercise
ChIP-seq: H3K27Ac
3955 enhancer regions
4095 associated genes
B
TSS
Region-gene association (%)
174
1621
1127
105
107
1539
2615
257
<-500
-500 to -50
-50 to-5
-5 to 0
0 to 5
5 to 50
50 to 500
>500
Distance from TSS (kb)
E
WT Mice
6-wks Old
Sedentary
Exercise
ChIP-seq: MEF2
10032 enhancer regions
9277 associated genes
F
TSS
Region-gene association (%)
319
3171
2383
3463
3040
3357
4592
393
Distance from TSS (kb)
C
GO Molecular Function
-log10(Binomial p value)
kinase binding 27.40
protein kinase binding 25.69
insulin-like growth factor receptor binding 17.75
integrin binding 16.17
coreceptor activity 9.73
kinase regulator activity 9.22
3',5'-cyclic-nucleotide phosphodiesterase activity 8.02
protease binding 7.49
phosphoric diester hydrolase activity 7.33
collagen binding 6.85
chemokine activity 6.49
small conjugating protein binding 6.12
fibroblast growth factor binding 5.86
chemokine receptor binding 5.65
vitamin transmembrane transporter activity 2.95
G
GO Molecular Function
-log10(Binomial p value)
ATPase binding 13.00
cAMP binding 11.80
cyclic nucleotide binding 9.43
cyclic-nucleotide phosphodiesterase activity 7.25
monovalent cation:hydrogen antiporter activity 2.67
D
GO Biological Process
-log10(Binomial p value)
apoptotic signaling pathway 27.96
negative regulation of protein phosphorylation 25.49
regulation of apoptotic signaling pathway 24.48
negative regulation of phosphorylation 24.33
positive regulation of apoptotic signaling pathway 24.07
negative regulation of protein modification process 24.04
positive regulation of cellular component movement 23.16
response to cytokine stimulus 22.57
positive regulation of cell migration 22.24
positive regulation of cell motility 21.94
negative regulation of phosphate metabolic process 19.39
regulation of glucose metabolic process 19.13
negative regulation of kinase activity 18.86
gland morphogenesis 18.47
branching involved in prostate gland morphogenesis 18.07
negative regulation of transferase activity 18.00
regulation of carbohydrate biosynthetic process 17.52
extrinsic apoptotic signaling pathway 17.32
cell-type specific apoptotic process 17.19
negative regulation of intracellular protein kinase cascade 17.16
H
GO Biological Process
-log10(Binomial p value)
cellular response to peptide hormone stimulus 19.47
cellular response to insulin stimulus 15.43
signal transduction by p53 class mediator 11.89
cAMP catabolic process 9.71
cyclic nucleotide catabolic process 9.66
regulation of fatty acid oxidation 9.57
regulation of potassium ion transmembrane transporter activity 9.08
organelle transport along microtubule 6.48
negative regulation of cytokine biosynthetic process 5.21
cardiac myofibril assembly 4.83
positive regulation of steroid metabolic process 4.65
commissural neuron axon guidance 4.62
negative regulation of transporter activity 4.58
organic cation transport 3.68
positive regulation of lipopolysaccharide-mediated signaling pathway 3.40
macrophage differentiation 2.78
positive regulation of endothelial cell apoptotic process 2.57
apoptotic process involved in patterning of blood vessels 2.15
I
GO Molecular Function
-log10 (p-value)
protein binding
anion binding
ion binding
carbohydrate derivative binding
kinase binding
transferase activity, transferring phosphorus containing groups
protein kinase binding
growth factor binding
phosphotransferase activity, alcohol group as acceptor
adenyl ribonucleotide binding
J
Sedentary
1kb
Exercise
Nr4a2/Nurr1
Exon 1
Exon 3

Fig. S1. Chromatin-associated H3K27Ac and MEF2 during exercise.

(*A*) Schematic of H3K27Ac ChIP-seq experiments on tibialis anterior muscle isolated from sedentary mice or mice following 8-weeks of voluntary wheel-running. A total 3,955 H3K27Ac peaks enriched with exercise were associated with 4,095 genes. (*B*) Distance of H3K27ac ChIP-seq peaks from associated genes. Numbers of genes within the indicated distances in kilobases are shown. TSS, transcription start site. (*C*) Gene ontology (GO) molecular function analysis of genes associated with H3K27Ac peaks in response to exercise. (*D*) Gene ontology (GO) biological process analysis of genes associated with H3K27Ac peaks in response to exercise. (*E*) Schematic of MEF2 ChIP-seq experiments on tibialis anterior muscle isolated from sedentary mice or mice following 8-weeks of voluntary wheel-running. A total 10,032 MEF2 peaks enriched with exercise were associated with 9,277 genes. (*F*) Distance of ChIP-seq peaks from associated genes.

(*G*) Gene ontology (GO) molecular function analysis of genes associated with MEF2 peaks in response to exercise. (*H*) Gene ontology (GO) biological process analysis of genes associated with MEF2 peaks in response to exercise. (*I*) Gene ontology (GO) molecular function analysis of genes associated with H3K27Ac and MEF2 peaks in response to exercise. (*J*) MEF2 ChIP-seq peaks at the *Nr4a2/Nurr1* locus from muscle of sedentary and exercised mice.

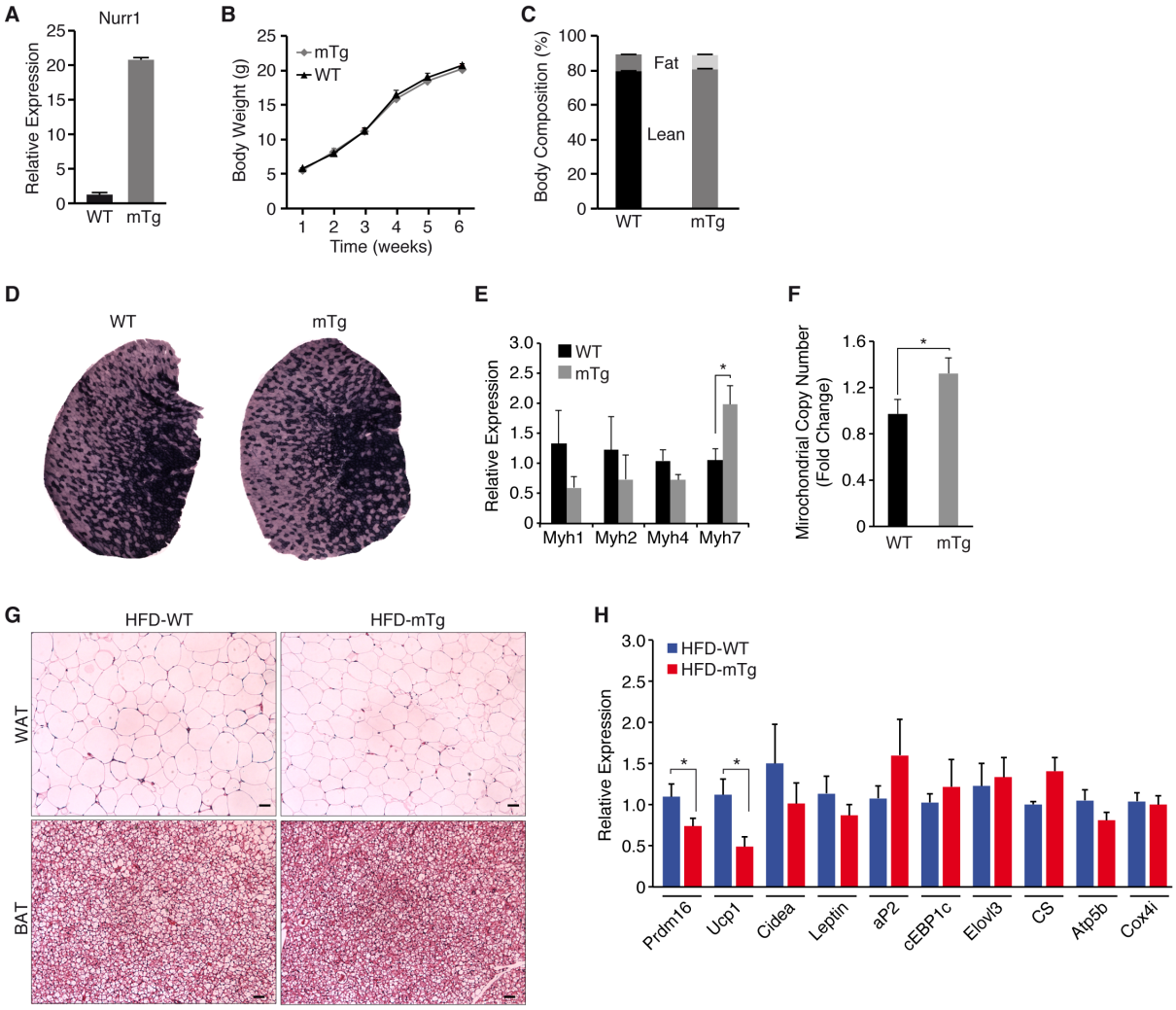

Fig. S2. Comparison of *Nurr1*-mTg and WT mice. (*A*) Expression of *Nurr1* mRNA normalized to 18S RNA in skeletal muscle of adult WT and *Nurr1*-mTg (mTg) mice, as detected by qRT-PCR. (*B*) Weekly body weight measurements on normal chow beginning at 6 weeks of age. (*C*) Body composition of WT and *Nurr1*-mTg mice on normal chow at 8 weeks of age. (*D*) Succinate dehydrogenase staining of tibialis anterior muscle. (*E*) Expression of myosin heavy chain genes normalized to 18S RNA in gastrocnemius muscle, as detected by qRT-PCR. (*F*) Mitochondrial copy number in muscle from adult WT and *Nurr1*-mTg mice. (*G*) H&E staining of white adipose tissue (WAT) and brown adipose tissue (BAT) from adult WT and *Nurr1*-mTg mice on HFD. Scale bar, 50 μm. (*H*) Expression of the indicated genes normalized to 18S RNA in WAT from adult WT and *Nurr1*-mTg mice. Data are represented as mean ± SEM. (n=8) *P< 0.05.

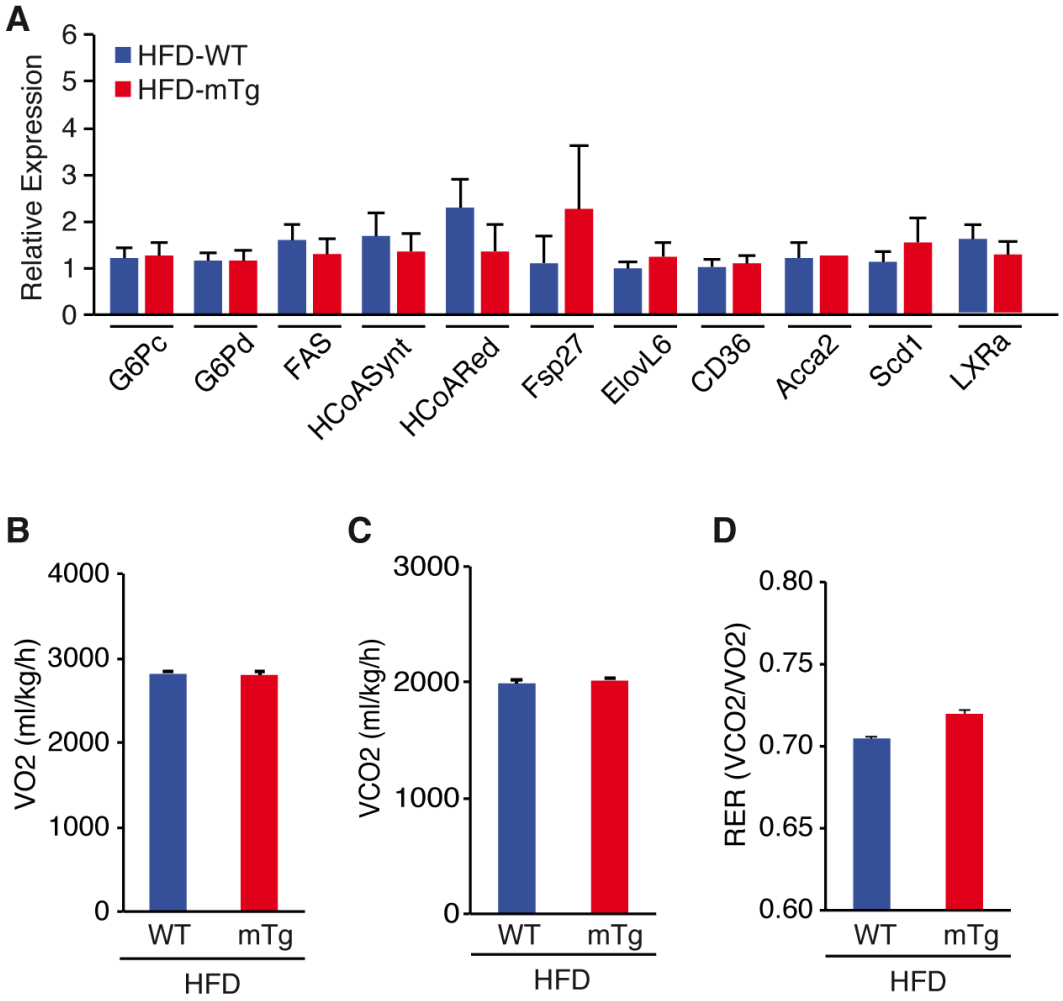

Fig. S3. Whole body energy expenditure and gene expression changes in liver from mice on HFD for 10 weeks. (*A*) Expression of genes involved in fatty acid transport (*CD36/FATP*) and synthesis (*Fsp27*), fatty acid biosynthesis (*Scd1*; *Fas*; *Elovl6*; *Acca2*), cholesterol synthesis (*HCoASynt*; *HCoARed*; *Pcsk9*), gluconeogenesis (*G6Pc*; *G6Pd*) and liver X receptor (*LXR*) normalized to 18S RNA in liver. (*B*) Twelve-week-old male *Nurr1*-mTg and WT mice on HFD were analyzed in metabolic cages over 4.5 days. Average oxygen consumption per hour during the light/dark cycle was normalized to lean mass. (*C*) Average carbon dioxide production per hour during the light/dark cycle normalized to lean mass. (*D*) Respiratory exchange rates (RER). Data are represented as mean ± SEM. (n = 8).

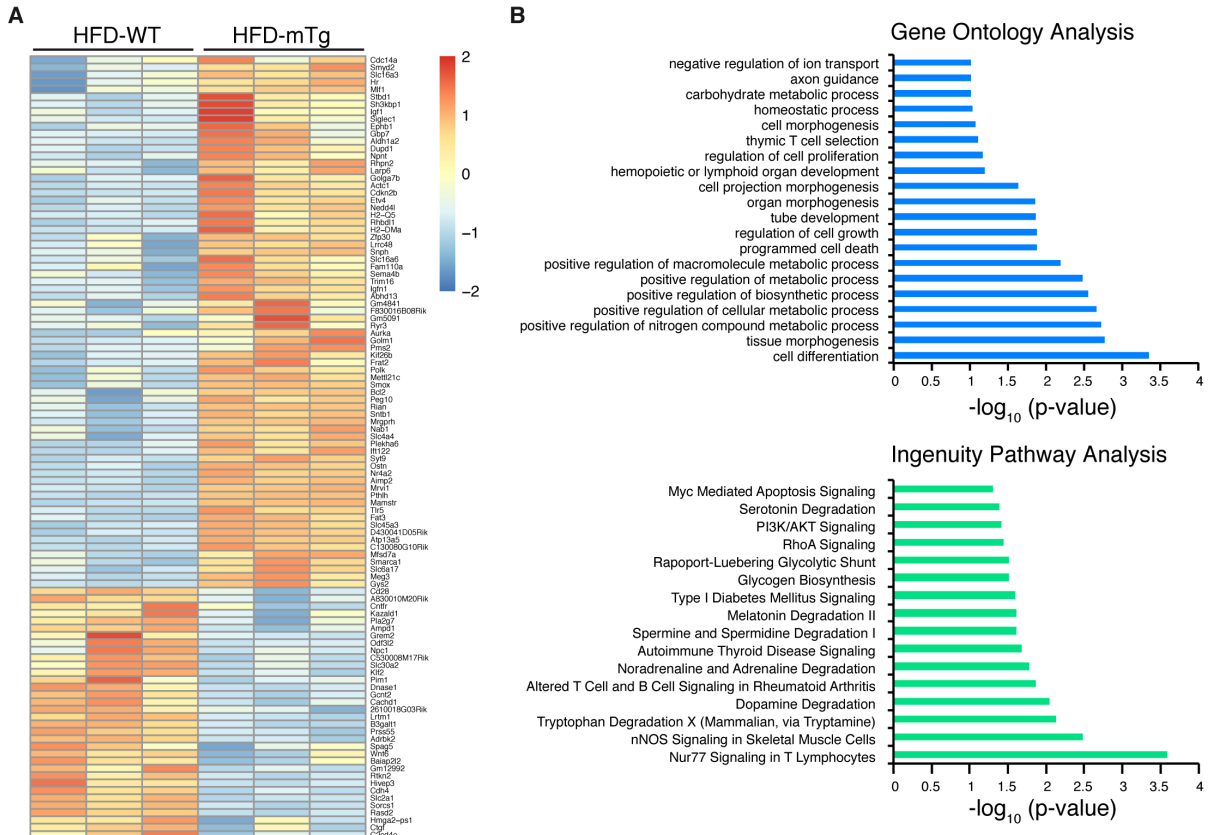

Fig. S4. Overall changes in skeletal muscle gene expression in *Nurr1*-mTg mice. (*A*) Heat map of differentially expressed genes from Illumina RNA-seq analysis comparing RNA isolated from gastrocnemius muscle of 6-week old *Nurr1*-mTg and WT mice after 10 weeks on HFD. The heat maps represent 3 biological replicates of each genotype. (*B*) Gene ontology and Ingenuity pathway analysis was used to reveal the top cellular and molecular networks.

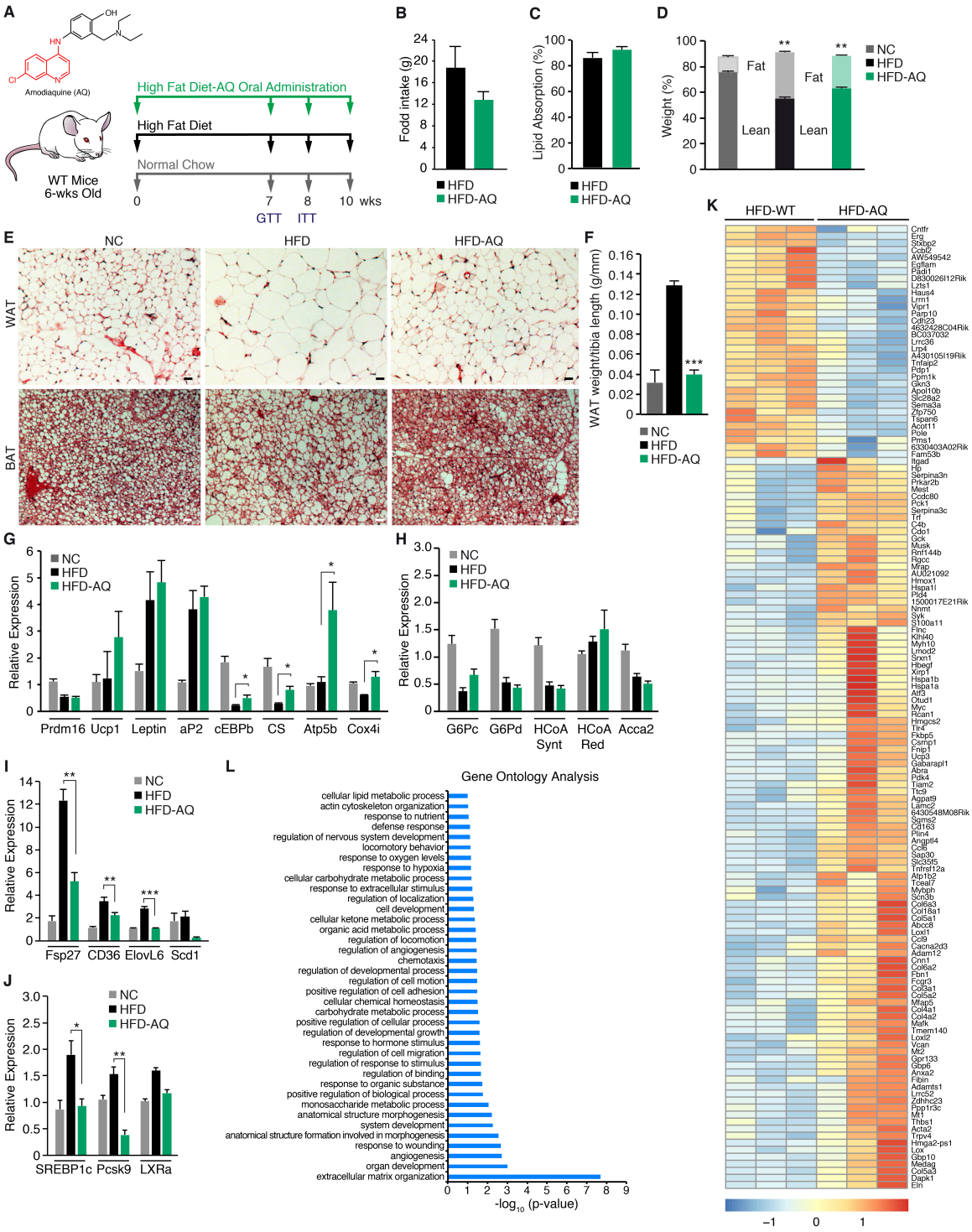
A
Amodiaquine (AQ)
High Fat Diet-AQ Oral Administration
High Fat Diet
Normal Chow
WT Mice
6-wks Old
0
7
8
10 wks
GTT
ITT
B
Fodd intake (g)
HFD
HFD-AQ
C
Lipid Absorption (%)
HFD
HFD-AQ
D
Weight (%)
Fat
Lean
Fat
Lean
NC
HFD
HFD-AQ
E
NC
HFD
HFD-AQ
WAT
BAT
F
WAT weight/tibia length (g/mm)
NC
HFD
HFD-AQ
G
Relative Expression
NC
HFD
HFD-AQ
Prdm16
Ucp1
Leptin
aP2
cEBPb
CS
Atp5b
Cox4i
H
Relative Expression
NC
HFD
HFD-AQ
G6Pc
G6Pd
HCoA Synt
HCoA Red
Acca2
I
Relative Expression
NC
HFD
HFD-AQ
Fsp27
CD36
ElovL6
Scd1
J
Relative Expression
NC
HFD
HFD-AQ
SREBP1c
Pcsk9
LXRa
K
HFD-WT
HFD-AQ
L
Gene Ontology Analysis
cellular lipid metabolic process
actin cytoskeleton organization
response to nutrient
defense response
regulation of nervous system development
locomotory behavior
response to oxygen levels
response to hypoxia
cellular carbohydrate metabolic process
response to extracellular stimulus
regulation of localization
cell development
cellular ketone metabolic process
organic acid metabolic process
regulation of locomotion
regulation of angiogenesis
chemotaxis
regulation of developmental process
regulation of cell motion
positive regulation of cell adhesion
cellular chemical homeostasis
carbohydrate metabolic process
positive regulation of cellular process
regulation of developmental growth
response to hormone stimulus
regulation of cell migration
regulation of response to stimulus
regulation of binding
response to organic substance
positive regulation of biological process
monosaccharide metabolic process
anatomical structure morphogenesis
system development
anatomical structure formation involved in morphogenesis
response to wounding
angiogenesis
organ development
extracellular matrix organization
-log10 (p-value)

Fig. S5. Decreased adiposity in mice orally treated with AQ for 10 weeks on HFD.

(*A*) Regimen for treatment of mice with AQ in the drinking water for 10 weeks. Glucose tolerance tests (GTT) and insulin tolerance tests (ITT) were performed after 7 and 8 weeks, respectively. (*B*) Food intake of mice on HFD in the absence or presence of AQ. Values were measured daily over a week. (*C*) Lipid absorption of mice on HFD in the presence or absence of AQ. Total dietary lipid absorption was evaluated over 72 hours. (*D*) Body composition of mice on normal chow (NC) or HFD in the absence or presence of AQ following 10-weeks of HFD. (*E*) H&E staining of white adipose tissue (WAT) and brown adipose tissue (BAT) from mice on normal chow (NC), HFD or HFD after 10 weeks of AQ treatment (HFD-AQ). (*F*) WAT weight normalized to tibia length in WT mice on normal chow (NC), HFD, or HFD with AQ treatment for 10 weeks (HFD-AQ). (*G*) Expression of marker genes of BAT (*Ucp1*; *Prdm16*), adipogenesis (*Leptin*, *aP2; cEBP1c*) and mitochondrial gene expression (*CS*; *Atp5b*; *Cox4i*) in WAT from WT mice on normal chow (NC), HFD, or HFD with AQ treatment for 10 weeks (HFD-AQ). (*H*) Expression of genes involved in gluconeogenesis (glucose 6-phosphatase c, *G6Pc*; glucose 6-phosphatase d, *G6Pd*), cholesterol synthesis (HMG-CoA-synthase, *HCoASynt*; HMG-CoA-reductase, *HCoARed*) and fatty acid biosynthesis (acetyl-CoA carboxylase alpha, *Acca2*) from WT mice on normal chow (NC), HFD, or HFD with AQ treatment for 10 weeks (HFD-AQ). (*I* and *J*) Expression of genes involved in fatty acid transport (*CD36/FATP*) and synthesis (*Fsp27*, *Scd1*; *Elovl6*), liver lipid metabolism (sterol regulatory element binding transcription factor 1c (SREBP1c), proprotein convertase subtilisin/kexin type 9, *Pcsk9*) and liver X receptor (*LXR*) in liver from WT mice on normal chow (NC), HFD, or HFD with AQ treatment for 10 weeks (HFD-AQ). (*K*) Heat map of differentially expressed genes in muscle of WT mice on HFD in response to AQ. The heat maps represent 3 biological replicates of WT mice on HFD in the absence or presence of AQ. (*L*) Gene ontology pathway analysis was used to reveal the top cellular and molecular networks. Data are represented as mean ± SEM. (n=8). Scale bar, 50 μm. **P*< 0.05; ***P*< 0.005; ****P*< 0.0005.

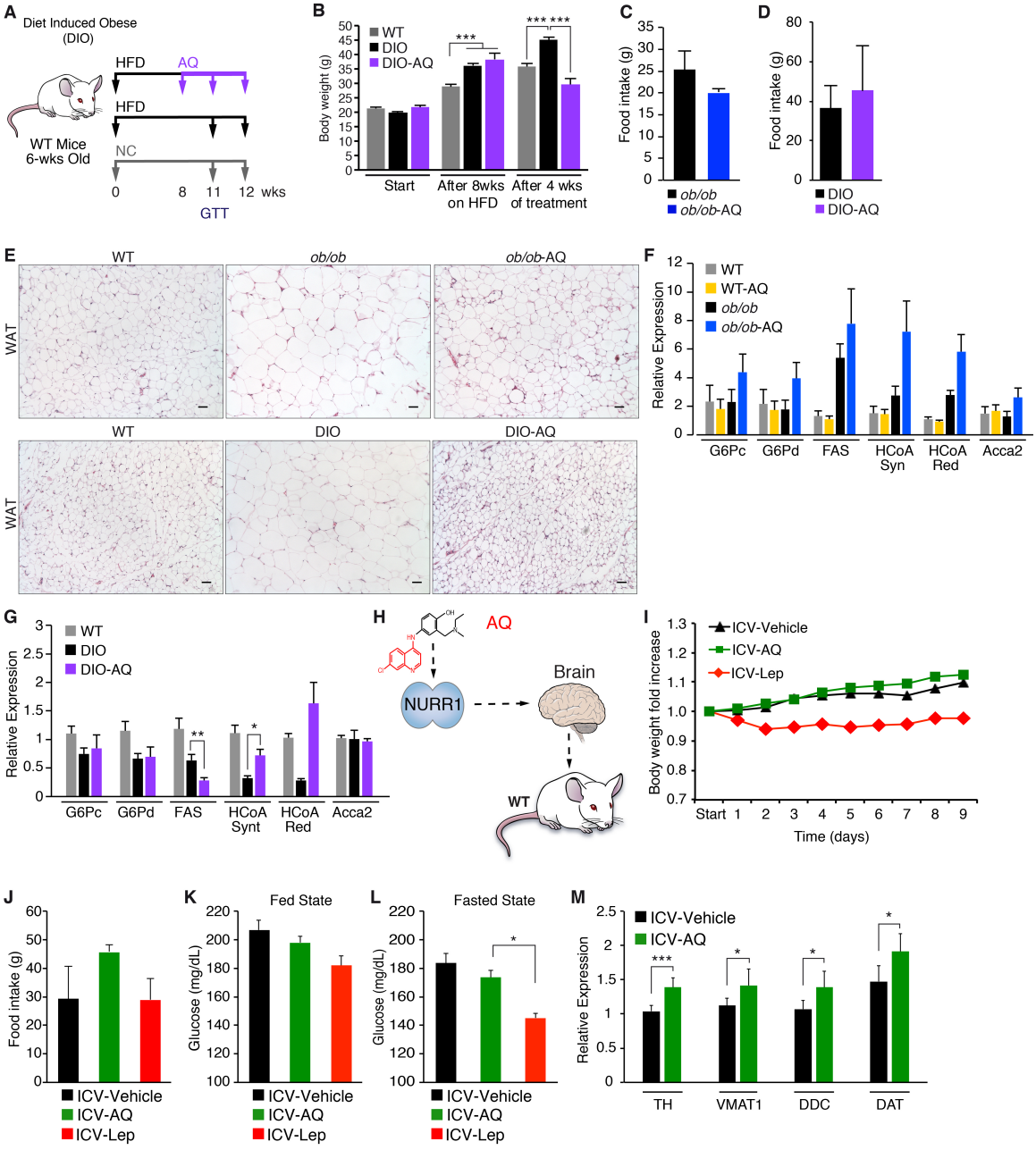
A
Diet Induced Obese (DIO)
HFD
AQ
HFD
NC
WT Mice 6-wks Old
0
8
11
12 wks
GTT
B
WT
DIO
DIO-AQ
Body weight (g)
***
*** ***
Start
After 8wks on HFD
After 4 wks of treatment
C
Food intake (g)
ob/ob
ob/ob-AQ
D
Food intake (g)
DIO
DIO-AQ
E
WT
ob/ob
ob/ob-AQ
WAT
WT
DIO
DIO-AQ
WAT
F
WT
WT-AQ
ob/ob
ob/ob-AQ
Relative Expression
G6Pc
G6Pd
FAS
HCoA Syn
HCoA Red
Acca2
G
WT
DIO
DIO-AQ
Relative Expression
**
*
G6Pc
G6Pd
FAS
HCoA Synt
HCoA Red
Acca2
H
AQ
NURR1
Brain
WT
I
ICV-Vehicle
ICV-AQ
ICV-Lep
Body weight fold increase
Start
Time (days)
J
Food intake (g)
ICV-Vehicle
ICV-AQ
ICV-Lep
K
Fed State
Glucose (mg/dL)
ICV-Vehicle
ICV-AQ
ICV-Lep
L
Fasted State
Glucose (mg/dL)
*
ICV-Vehicle
ICV-AQ
ICV-Lep
M
ICV-Vehicle
ICV-AQ
Relative Expression
***
*
*
*
TH
VMAT1
DDC
DAT

Fig. S6. Effect of AQ treatment on *ob/ob*, DIO and WT mice. (*A*) Regimen for WT mice at 6 weeks of age on high fat diet (HFD) induced obesity (DIO) study in the absence or presence of AQ for 4 weeks. Normal chow; NC. (*B*) Body weight of WT, DIO and DIO mice administered AQ (DIO-AQ) at the start (6 weeks of age) and the end (12 weeks of age) of the experiment. (*C* and *D*) Food intake of WT and (*C*) *ob/ob* and (*D*) DIO mice in the absence or presence of AQ. Values were measured daily over one week. (*E*) H&E staining of white adipose tissue (WAT) from untreated WT, *ob/ob* or DIO mice compared to *ob/ob* or DIO mice treated orally with AQ (*ob/ob*-AQ or DIO-AQ) for 4 weeks. (*F* and *G*) Gene expression changes in liver tissue from WT, (*F*) *ob/ob* and (*G*) DIO mice treated or untreated with AQ for 4 weeks. Expression of genes involved in gluconeogenesis (*G6Pc*; *G6Pd*), fatty acid biosynthesis (*Fas*; *Acca2*) and cholesterol synthesis (*HCoASynt*; *HCoARed*) in liver tissue. (*H*) Schematic of intracerebroventricular (ICV) administration of AQ for 2 weeks to WT mice on HFD at 6 weeks of age. (*I*) Daily body weight measurement of WT mice on HFD with vehicle, AQ or leptin administered by ICV. (*J*) Food intake of WT mice on HFD with vehicle, AQ or leptin administered by ICV. (*K*) Glucose serum levels in fed state of WT mice on HFD with vehicle, AQ or leptin administered by ICV. (*L*) Glucose serum levels in fasted state of WT mice on HFD with vehicle, AQ or leptin administered by ICV. (*M*) Expression of genes responsive to *Nurr1* activation in WT mice at 6 weeks of age on HFD with vehicle or AQ administered by ICV for 2 weeks. Tyrosine Hydroxylase, *TH*; Vesicular Amine Transporter 1, *VMAT1*; Dopa Decarboxylase, *DDC*; and Dopamine Transporter, *DAT*. Data are represented as mean ± SEM. Scale bar, 50 μm. (n=5) *P< 0.05; **P< 0.005; ***P< 0.0005.

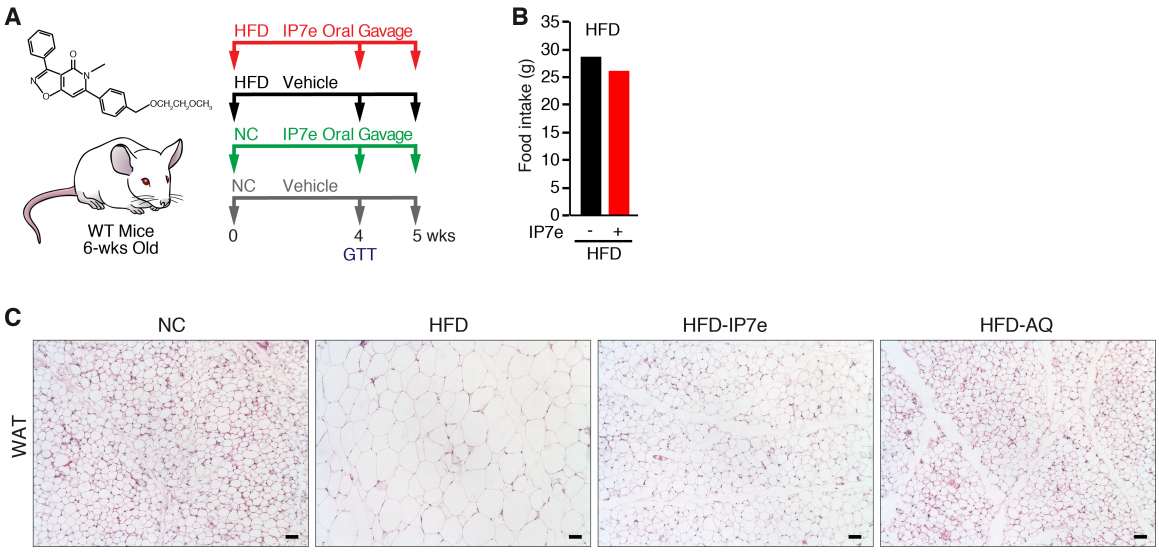

Fig. S7. Decreased adiposity in WT mice on HFD treated with IP7e.

(*A*) Regimen for treatment of mice with IP7e. WT mice on HFD or NC diet were treated with IP7e for 5 weeks. Glucose tolerance test (GTT) was performed 4 weeks after IP7e treatment. (*B*) Food intake of mice on HFD in the absence or presence of IP7e. Values were measured daily over one week. (*C*) H&E staining of white adipose tissue (WAT) from mice under the indicated conditions. IP7e and AQ treatment was for 4 weeks. Scale bar, 50 μm.

Table S1: Mouse primers for qPCR and ChIP assay

Experiment	Primer name	Sequence (5' to 3')
qPCR	Fsp27-Fw	TCGACCTGTACAAGCTGAACCCT
qPCR	Fsp27-Rv	AGGTGCCAAGCAGCATGTGACC
qPCR	CD36-Fw	TTAGATGTGGAACCCATAACTGGA
qPCR	CD36-Rv	TTGACCAATATGTTGACCTGCAG
qPCR	SREBP1c-Fw	GGAGCCATGGATTGCACATT
qPCR	SREBP1c-Rv	GGCCCGGGAAGTCACTGT
qPCR	PCSK9-Fw	TGCGTGTGCTCAATGTCAA
qPCR	PCSK9-Rv	GATTAGCTGACTCTTCCGAATAAACTC
qPCR	LXRa-Fw	AGGAGTGTCGACTTCGCAAA
qPCR	LXRa-Rv	CTCTTCTTGCCGCTTCAGTTT
qPCR	Glut4-Fw	TTGGCTCCCTTCAGTTTGG
qPCR	Glut4-Rv	CTACCCAGCCACGTTGCAT
qPCR	Glut1-Fw	CGCCCCCCAGAAGGTTAT
qPCR	Glut1-Rv	CGATGCGGTGGTTCCAT
qPCR	G6Pd-Fw	ACCTTGCGGCTCACTTTCC
qPCR	G6Pd-Rv	GAAAGTTTCAGCCACAGCAATG
qPCR	Nr4a2-Fw	TGTCGTAATTCAGCGAAGGA
qPCR	Nr4a2-Rv	TGAATGAAGAGAGCGGACAA
qPCR	Ucp1-Fw	GTGAACCCGACAACTTCCGAA
qPCR	Ucp1-Rv	TGAAACTCCGGCTGAGAAGA T
qPCR	Cidea-Fw	TGCTCTTCTGTATCGCCCAGT
qPCR	Cidea-Rv	GCCGTGTTAAGGAATCTGCTG
qPCR	aP2-Fw	GATGCCTTTGTGGGAACCTG
qPCR	aP2-Rv	TCCTGTCGTCTGCGGTGATT
qPCR	Leptin-Fw	TGAAGCCCAGGAATGAAGTC
qPCR	Leptin-Rv	TCAAGACCATTGTCACCAGG
qPCR	cEBP1c-Fw	GCACAAGGTGCTGGAGCTGAC
qPCR	cEBP1c-Rv	CTTGAACAAGTTCCGCAGGGT
qPCR	Elovl3-FW	TCCGCGTTCTCATGTAGGTCT
qPCR	Elovl3-Rv	GGACCTGATGCAACCCTATGA
qPCR	CS-Fw	GGACAATTTTCCAACCAATCTGC
qPCR	CS-Rv	TCGGTTCATTCCCTCTGCATA
qPCR	Atp5b-Fw	CTCTGACTGGTTTGACCGTTGC
qPCR	Atp5b-Rv	TGGTAGCCTACAGCAGAAGGGA
qPCR	Cox4i-Fw	AGTGTTGTGAAGAGTGAAGAC

qPCR	Cox4i-Rv	GCGGTACAACTGAACTTTCTC
qPCR	G6Pd-Fw	ACCTTGCGGCTCACTTTCC
qPCR	G6Pd-Rv	GAAAGTTTCAGCCACAGCAATG
qPCR	G6Pc-Fw	GTGGCAGTGGTCGGAGACT
qPCR	G6Pc-Rv	ACGGGCGTTGTCCAAAC
qPCR	FAS-Fw	GCTGCGGAAACTTCAGGAAAT
qPCR	FAS-Rv	AGAGACGTGTCACTCCTGGACTT
qPCR	HMG-CoA-synt-Fw	GCCGTGAACTGGGTCGAA
qPCR	HMG-CoA-synt-Rv	GCATATATAGCAATGTCTCCTGCAA
qPCR	HMG-CoA-red-Fw	CTTGTGGAATGCCTTGTGATTG
qPCR	HMG-CoA-red-Rv	AGCCGAAGCAGCACATGAT
qPCR	Elovl6-Fw	AAGCCACGAAGGCTGAGTAG
qPCR	Elovl6-Rv	TGCCTGCTCATACGGATGTTT
qPCR	CD36-Fw	TTAGATGTGGAACCCATAACTGGA
qPCR	CD36-Rv	TTGACCAATATGTTGACCTGCAG
qPCR	Acaa2-Fw	GATCTCAAGCTGGAAGATAC
qPCR	Acaa2-Rv	ACCTCTGCTGAGACTGCAAG
qPCR	SCD-1-Fw-LA	TGCCCCTGCGGATCTT
qPCR	SCD-1-rv-LA	GCCCATTCGTACACGTCATT
qPCR	18s-Fw	ACCGCAGCTAGGAATAATGGA
qPCR	18s-Rv	GCCTCAGTTCCGAAAACCA
qPCR	LXRa-Fw	AGGAGTGTCGACTTCGCAAA
qPCR	LXRa-Rv	CTCTTCTTGCCGCTTCAGTTT
qPCR	Myh1	TAQMAN PROBE: MM01332489_G1
qPCR	Myh2	TAQMAN PROBE: MM01332564_M1
qPCR	Myh4	TAQMAN PROBE: MM01332518_M1
qPCR	Myh7	TAQMAN PROBE: MM01319006_G1
qPCR	Prdm16	TAQMAN PROBE: MM00712556_M1
ChIP assay	Glut4 promoter-Fw	AGGACCCCACTTTGAAATCC
ChIP assay	Glut4 promoter-Rv	AAGGCTCTCCGGGATCTAAT